J Therm Anal Calorim (2015) 120:1563–1571
DOI 10.1007/s10973-015-4518-z

Decreased thermal diffusivity in fluids containing InP nanocrystals

J. F. Sánchez Ramírez · S. F. Arvizu Amador · J. L. Jiménez Pérez · A. Bautista Hernández · R. J. Delgado Macuil · J. Díaz Reyes · E. Chigo Anota

Received: 5 November 2014 / Accepted: 31 January 2015 / Published online: 3 March 2015

Abstract Colloidal suspensions of semiconductor InP nanocrystals were prepared using the reaction of indium myristate and tris(trimethylsilyl)phosphine in 1-octadecene at elevated temperatures. The semiconductor nanocrystals are highly crystalline, monodisperse and soluble in various organic solvents. Thermal properties of toluene containing 4.6 nm InP semiconductor with different percentage mass (6.0–16.0 %) were measured using the mode-mismatched dual-beam thermal lens technique. This was performed to determine the effect on nanofluids' thermal diffusivity caused by the presence and concentration of semiconductor nanocrystals. The characteristic time constant of the transient thermal lens was estimated by fitting the experimental data to the theoretical expression for transient thermal lens to determine the thermal diffusivity of the semiconductor nanofluids (toluene containing InP nanocrystals). The results obtained show that the nanofluids' thermal diffusivity depends strongly on the contents of the nanocrystals. The thermal diffusivity enhancement in nanofluids is negative when concentration of nanocrystals increases. Such behavior differs from other nanofluids, since they have shown positive thermal diffusivity enhancements. The minimum diffusivity was achieved on nanofluids with higher concentrations. A possible explanation for such low thermal diffusivity of the nanofluids with semiconductor nanocrystals is given. In order to characterize the InP nanocrystals, the following techniques were used: UV–Vis spectroscopy, transmission electron microscopy and high-resolution electron microscopy.

Keywords Thermal diffusivity · Thermal lens · Nanofluids · Semiconductor nanocrystals · InP nanoparticles

J. F. Sánchez Ramírez (✉) · R. J. Delgado Macuil · J. Díaz Reyes
CIBA-Instituto Politécnico Nacional, San Juan Molino Km 1.5 de la Carretera Estatal Sta. Inés Tecuexcomac-Tepetitla, Tlaxcala 90700, México
e-mail: jfsanchez@ipn.mx

S. F. Arvizu Amador · J. L. Jiménez Pérez
UPIITA-Instituto Politécnico Nacional, Av. Instituto Politécnico Nacional 2580. Barrio Laguna Ticomán, 07340 México, D.F., México

A. Bautista Hernández
Facultad de Ingeniería, Benemérita Universidad Autónoma de Puebla, Apartado Postal J-39, Puebla, Pue. 72570, México

E. Chigo Anota
Facultad de Ingeniería Química, Benemérita Universidad Autónoma de Puebla, Edificio 106E, C. U. San Manuel, C. P. 72570 Puebla, México

Introduction

After their variations of thermal properties were reported at the end of last century [1], nanofluids (which are mixture of solid nanoparticles in a liquid) are new compound liquids that had obtained a lot of interest [2–5]. Small amount of nanoparticles has significantly increased thermal conductivity of liquids such as water, ethylene glycol and oil when they are dispersed in these liquids. Although research studies on the thermal transport properties of nanofluids have been extensively performed [6–9], these have been limited to study of the enhanced thermal conductivity of nanofluids containing different types of nanoparticles such as oxides, pure metallic and carbon nanotubes using different techniques [10–15]. Thermal diffusivity is key to evaluate its thermal performance under flow conditions and in convective heat transfer-based applications, and despite

this, very few efforts have been made to determine it. In recent years, we have seen an increasing interest in the measurement and modeling of the thermal diffusivity properties in fluid suspensions containing nanometer-sized metallic particles [16–19]. However, semiconductor crystals are expected to significantly modify liquid's thermal diffusivity behavior due to the ability of tailoring their nanometer size [20]. The thermal properties of the semiconductor nanocrystals could deviate substantially from the bulk value due to the larger surface to volume ratio and explicit surface reconstruction effects, which could lead possibly to phonon scattering and confinement, especially at small diameters [21, 22]. A dramatic decrease in the thermal transport (conductivity) of semiconductor nanoparticles, as the particle size becomes from the same order as the phonon mean free path, has been very recently observed [23]. This interesting thermal behavior was used to obtain nanofluids, which exhibit negative thermal transport enhancements or a decrease in the effective thermal conductivity of the dispersion compared with that of the base liquid. This behavior is different from the other nanofluids, which have been shown to exhibit positive thermal transport enhancement.

The interest in nanofluids containing semiconductor nanocrystals is fueled by their significant potential in various technological applications such as DNA tagging or aqueous monitoring for biological and chemical changes in a given environment, targeting thermal agents in medical therapies with extended precision of thermal effects below cellular dimensions [24, 25]. With this motivation, in this work, we report measurement of the thermal diffusivity of semiconductor nanofluids in order to determine the effect of the presence of semiconductor nanocrystals and concentration of InP on the thermal diffusivity (D_N) of semiconductor nanofluids. Thermal diffusivity measurements are carried out in toluene containing 4.6 nm InP nanoparticles with different concentration using the thermal lens spectroscopy (TLS) [26, 27]. This technique is a reliable photothermal alternative to measure thermal diffusivity of semiconductor nanofluids with high sensitivity, which is totally noninvasive, the experimental apparatus and the data analysis are rather simple, and it does not require any type of preparation of the sample and can be applied to a wide range of semitransparent materials from nanofluids to solids. We used the mode-mismatched dual-beam thermal lens technique to measure the thermal diffusivity of nanofluids containing semiconductor nanocrystals. To the best of our knowledge, there is no study on the determination of the negative thermal diffusivity of nanofluids containing InP nanocrystals with different percentage mass (6.0–16.0 %). Besides, the size and optical properties of the samples were investigated using UV–Vis spectroscopy, transmission electron microscopy (TEM) and high-resolution transmission electron microscopy (HRTEM) techniques.

Experimental

Sample preparation

In order to prepare the semiconductor nanofluids, the InP nanocrystals were first synthesized using a chemical synthesis process [28] and then dispersed in toluene. The samples were then subjected to ultrasonic processing to obtain uniform dispersion. Firstly, the precursor of indium (indium myristate, In(MA)) was prepared and 0.1 mmol of indium acetate ($InAc_3$) was mixed under inert atmosphere with 0.3 mmol of myristic acid and 7.0 mL of 1-octadecene (ODE) in a 50-mL three-neck flask equipped with a condenser. The mixture was heated to 100 °C during 2 h under vacuum to obtain an optically clear solution, backfilled with Ar gas and cooled down at room temperature.

In another 50-mL three-neck flask equipped with a condenser, 0.2 mmol of dodecanethiol (DDT), 0.2 mmol of tris(trimethylsilyl)phosphine ($P(TMS)_3$), 10 mL of ODE and 0.2 mmol of In(MA) were stirred under inert atmosphere. The mixture was then heated to 250 °C of temperature for 2 h, and the temperature was then decreased at room temperature. The colloidal dispersions of InP prepared are stable with 4.6 nm in average diameter. The nanocrystals were repeatedly purified with chloroform/methanol/acetone (1:1:10 vol:vol:vol) followed by centrifugation, to remove the starting materials and side products. In order to obtain nanofluids containing InP nanoparticles with different percentage mass, the colloidal dispersion was collected by centrifugation and subsequently dried in vacuum at 60 °C for 1 h. Finally, the black powder was dissolved in toluene to obtain different semiconductor nanoparticles concentrations (6.0, 8.0, 10.0, 12.0, 14.0 and 16.0 mass/%) and was placed in a quartz cuvette of 1 cm thick for the optical and thermal measurement. The semiconductor nanofluids were stable for months without significant changes in the spectral pattern. All the experiments were performed at room temperature and subjected to ultrasonic processing prior to each measurement.

All chemicals used were of analytical grade from Sigma-Aldrich Corporation (St. Louis, MO, USA), and they were used as received; HPLC water was used in all times to wash the laboratory equipment used in the preparation of the nanofluids system.

Characterization

Room-temperature optical absorption spectrum of the colloidal sample was recorded using an UV–Vis–NIR

scanning spectrophotometer (Shimadzu UV 3101PC double beam). For electron microscopy analysis, two microscopes, Jeol JEM200 and Tecnai 200 TEM, were used for the low magnification and high-resolution observations of the samples, respectively. HRTEM images were digitally processed by using filters in the Fourier space. For TEM observations, a drop of colloidal solution was spread on Formvar carbon deposited on copper microgrid and dried in vacuum.

Theory of thermal lens

The thermal lens (TL) effect of such nanofluids was based on their laser-induced heating and time-resolved monitoring on the thermal effects. The TL effect is caused by the deposition of heat via non-radiative decay processes after the laser beam, with Gaussian profile, which has been absorbed by the sample. In this situation, a transverse temperature profile, $\Delta T(r, t)$, is established in the sample. The temporal evolution $\Delta T(r, t)$ is scaled according to characteristic time constant:

$$t_c = \frac{\omega_e^2}{4D} \tag{1}$$

where ω_e is the excitation laser beam radius in the sample and D is the thermal diffusivity. Owing to $\Delta T(r, t)$, a temperature coefficient of the optical path length change, $\frac{ds}{dT} = \frac{dn}{dT}$ (for liquids) is generated, creating a lens-like optical element: the so-called TL effect. The propagation of a probe laser beam through this TL results in a variation of its on-axis intensity, which can be calculated using diffraction integral theory. In transient regime, an analytical expression can be obtained for the probe beam intensity, $I(t)$ [29]:

$$I(t) = I(0)\left[1 - \frac{\theta}{2}\tan^{-1}\left(\frac{2mV}{\left[(1+2m)^2+V^2\right]\frac{t_c}{2t}+1+2m+V^2}\right)\right]^2 \tag{2}$$

where

$$V = \frac{Z_1}{Z_c} \tag{3}$$

$$m = \left(\frac{\omega_p}{\omega_e}\right)^2 \tag{4}$$

$$\theta = -\frac{P_e A_e l_0}{k\lambda_p}\left(\frac{dn}{dt}\right)_p \tag{5}$$

In Eq. (2), $I(0)$ is the initial value of $I(t)$ when t is zero; θ is the thermally induced phase shift of the probe beam after its passing through the sample; Z_c (12.89 cm) is the confocal distance of the probe beam; and Z_1 (8.0 cm) is the distance from the probe beam waist to the sample, respectively. ω_p is the probe beam spot sizes in the sample; A_e is the optical absorption coefficient at the excitation beam wavelength λ_e; λ_p is the probe beam wavelength; l_0 is the sample thickness; and $\frac{dn}{dT}$ is the temperature dependence of the sample refractive index. Then, by fitting the equation of $I(t)$ (Eq. 2) to the experimental data, as a function of time (t), it is possible to obtain the nanofluid thermal diffusivity of the nanofluid (Eq. 1) from t_c and θ as adjustable parameters.

Figure 1 is the schematic representation of the TL experimental setup. The excitation laser is an Ar^+ laser, at $\lambda = 514$ nm, which was focused by a converging lens L_1 ($\omega_e = 40$ μm), and the sample was placed at the focal plane of the lens 1. M1 and M2 are mirrors. Exposure of the sample to the excitation beam was controlled by means of a shutter, which was connected directly to the trigger of a digital oscilloscope. A He–Ne laser probe beam of 4 mW was focused with a lens L_2. The probe beam (at an angle $\phi \approx 3.0°$ with the excitation beam) was incident on the sample and carefully centered to pass through the thermal lens to maximize the thermal lens signal. After passing through the sample, the probe beam is reflected by mirrors M3, M4 and M5 to a pinhole mounted before a photodiode or photodetector (D). A band-pass filter 1, at the He–Ne laser wavelength, was placed over the photodiode to prevent stray light from entering the photodetector. The spot size of the probe beam at the pinhole was 10 cm because of scattering by the sample, and the radius of the pinhole used here was 0.5 cm. The output of the photodiode was coupled to the digital oscilloscope. The magnitude of the thermal lens signal with time was recorded in a PC, and the

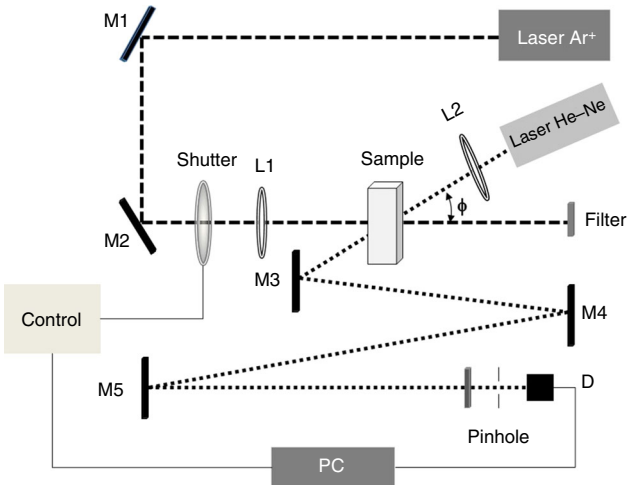

Fig. 1 Schematic representation of the thermal lens experimental setup

data thus obtained were fitting to Eq. (2) using least-squares curve fit to obtain the nanofluids' thermal diffusivity D_N (Eq. 1).

Results and discussion

To characterize the particles, TEM and HRTEM were used along with optical absorption spectroscopy to study the size, size distribution and fine structure of semiconductor InP colloids formed.

Figure 2 shows transmission electron micrograph of InP nanofluids with different percentage mass (8 and 12 %). As inset, distribution histogram and HRTEM images are presented. From this figure, we can observe the formation and size of the semiconductor particles. The particle shape was nearly spherical with sizes in the nanometer scale. The presence of clusters with an interparticle separation <2 nm is observed in the image. The clustering degree of nanoparticles differs from the increasing percentage mass of the nanoparticles, for example, when the percentage mass is 8 % (Fig. 2a), most nanoparticles are clustered; only very few nanoparticles are discrete. Increasing the concentration up to 12 %, more clustering with a size greater than 50 nm are formed (Fig. 2b). The formation of the clustering is related to distance and action force between the InP nanoparticles. Upon increasing the volume fraction of the nanoparticles, the distance decreases, while the action force increases, both favor the formation of the clustering. The size distributions followed a Gaussian fit with narrow size distributions (inset Fig. 2a); the average particle size is 4.6 nm with a standard deviation of 20 %, indicating that the nanocrystals are homogeneous due to separation nucleation and growth events during the reaction. The crystal size is smaller than the Bohr excitonic diameter (15 nm), belonging to a strongly quantum confined regime.

For closer observation on the crystallinity and fine structure of the nanocrystals, a HRTEM image of the sample was recorded. From the HRTEM images (Inset Fig. 2b), we can observe the formation of crystalline nanoparticles. Interplanar spacing calculated for the sample corresponds well with the interplanar spacing of the corresponding indium phosphide structures of the zinc-blende phase.

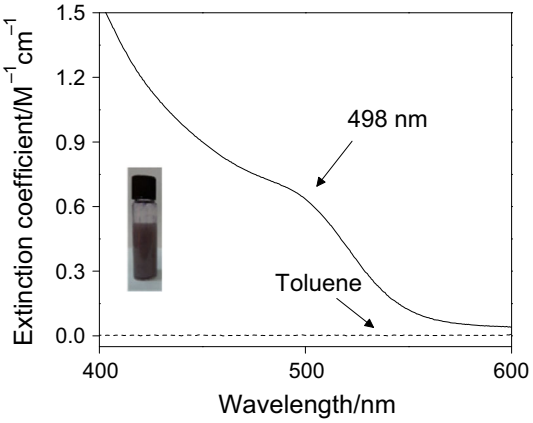

Fig. 3 Extinction coefficient of nanofluids consisting of InP nanoparticles dispersed in toluene. The *inset* shows the semiconductor nanofluids with 16.0 mass/% of InP nanoparticles

Formation of semiconductor nanocrystals was also confirmed from the UV–Vis absorption spectra. Nanocrystals such as InP in the nanoscale strongly absorb light when the excitation energy is greater than the bandgap energy. Figure 3 shows the absorption spectra of toluene containing InP nanocrystals obtained, and spectrum of toluene is also annexed as reference. All spectra were recorded at room temperature. From the figure, we can observe that an excitonic absorption peak appears at 498 nm. The absorption and TEM results are consistent with the previously reported relationship of particles size versus excitonic peak wavelength of InP nanoparticles [30, 31].

The time evolution of TL signal for the fluids containing semiconductor nanoparticles at different percentage mass

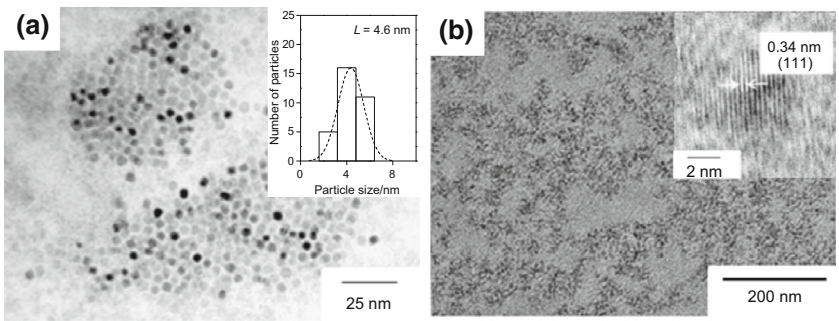

Fig. 2 TEM micrographs of InP nanofluids with different percentage mass: **a** 8 % and **b** 12 %, respectively. *Inset* (**a**): The normalized size distribution of particles of the semiconductor nanoparticles; average particles size (L) is calculated from Gaussian fitting of the histograms. *Inset* (**b**): Typical HRTEM images of semiconductor nanoparticles with phase zinc-blende with lattice spacing of 0.34 nm, respectively

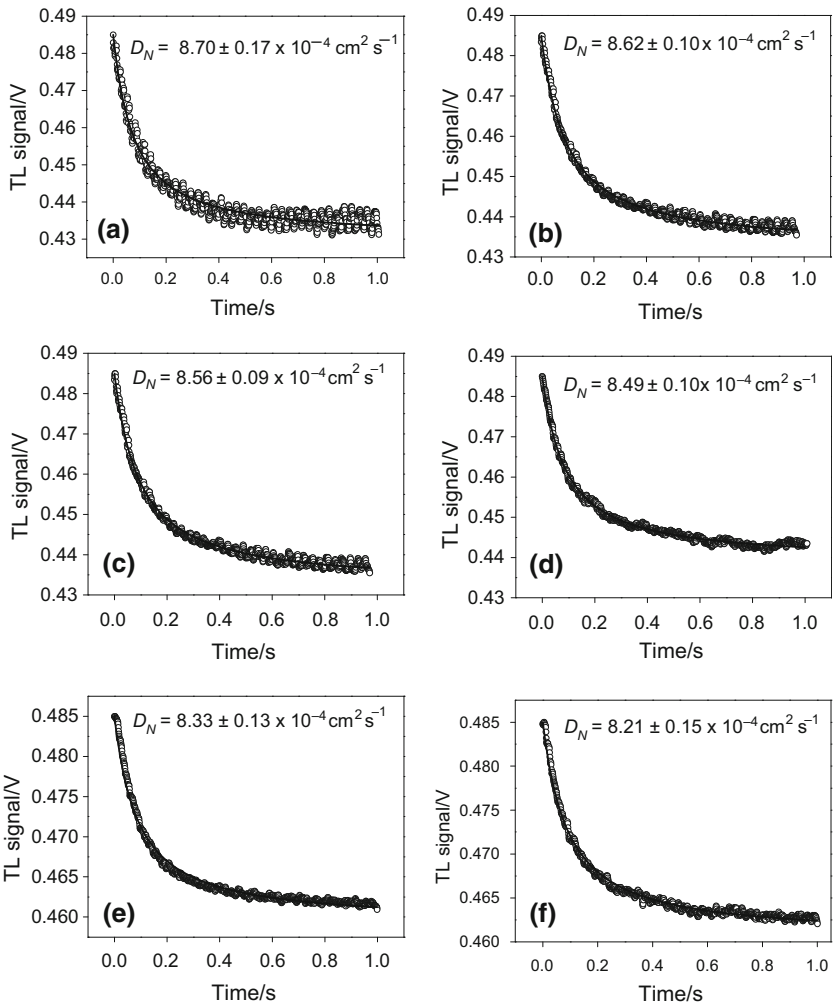

Fig. 4 Time evolution of TL signal semiconductor nanofluids with different percentage mass of nanoparticles semiconductor InP: **a** 6.0 %, **b** 8.0 %, **c** 10.0 %, **d** 12.0 %, **e** 14.0 % and **f** 16.0 %. Symbols (*open circle*) represent the experimental data, and solid line is the best fit to Eq. (2)

is shown in Fig. 4, where the symbols represent the experimental data points (o) and the solid lines correspond to their best fits to Eq. (2). It can be noted that the TL signal decreases as time elapses, indicating that the thermal lens are divergent, thus defocusing the probe beam on the detector. This behavior is because the temperature coefficient of the optical path length $\frac{ds}{dT}$ is negative for most of the transparent liquids and semitransparent materials as the plastics. In Table 1 shows, the adjustable parameters θ and t_c obtained from the best fit of Eq. (2) to TL experimental data and thermal diffusivity data of semiconductor nanofluids.

The results show that the thermal diffusivity of all the fluids containing semiconductor nanoparticles shows lower values with respect to the base liquid (toluene, $D_l = 10.4 \times 10^{-4}$ cm^2 s^{-1}) [26], so that the thermal diffusivity enhancement in semiconductor nanofluids is negative. This behavior is different that of the other nanofluids, which have been shown to exhibit positive thermal diffusivity enhancement [16–19, 27]. Figure 5 shows the dependency of the semiconductor nanofluid thermal diffusivity on nanoparticles concentration, as the nanoparticles concentration increases the thermal diffusivity decreased percentage of nanofluids. The minimum thermal diffusivity was obtained by the fluid containing higher concentrations of semiconductor nanoparticles. This interesting thermal behavior has not been explored yet; below we propose a probable explanation to interpret such results.

There are recent studies about thermal transport in semiconductor crystalline solids confined in the nanometer range where it is reported that the thermal properties of solid particles are of several orders of magnitude smaller than the corresponding bulk value [21, 22, 32]. These decreases were attributed to the altering phonon spectra of the materials in nanometric scale. Latter suggests that InP semiconductor particles confined in nanometric scale would also show heat transfer (thermal diffusivity) that is significantly less than the corresponding bulk value (0.43 cm^2 s^{-1}) [33] and than that of common liquids (i.e.,

Table 1 Adjustable parameters t_c y θ obtained from the best fit of Eq. (2) to TL experimental data and thermal diffusivity data of semiconductor nanofluids containing 4.6 nm InP nanocrystals with different percentage mass

Sample	Mass/%	$t_c/10^{-3}$ s	$\theta/10^{-2}$	$D_N/10^{-4}$ cm^2 s^{-1}
Toluene	–	–	–	10.40 [26]
1	6	4.65 ± 0.02	18.98 ± 0.053	8.71 ± 0.17
2	8	4.66 ± 0.02	9.22 ± 0.044	8.62 ± 0.10
3	10	5.04 ± 0.05	19.16 ± 0.055	8.56 ± 0.09
4	12	4.75 ± 0.03	16.66 ± 0.030	8.49 ± 0.10
5	14	4.79 ± 0.02	8.98 ± 0.046	8.33 ± 0.13
6	16	4.77 ± 0.02	8.77 ± 0.048	8.21 ± 0.15

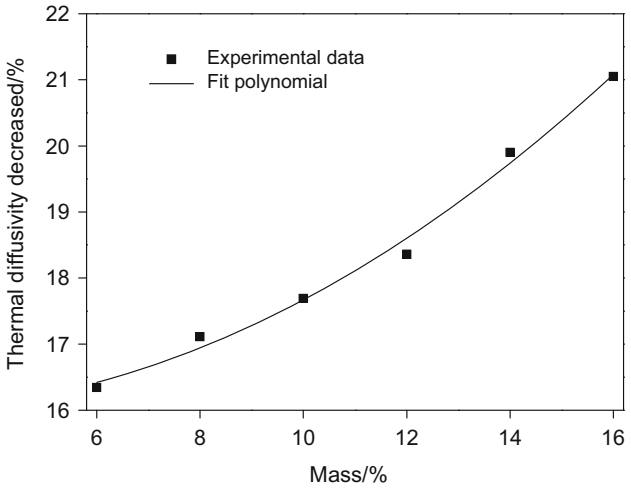

Fig. 5 Thermal diffusivity values of the samples of InP nanocrystals at different percentage mass dispersed in toluene. The symbols (*filled circle*) represent the obtained thermal diffusivity decreased, and the *solid line* corresponds to the best linear fitting of this thermal parameter

toluene). Then, we may hypothesize that when these semiconductor particles of InP confined at nanometer scale are dispersed in toluene, the effective thermal diffusivity of nanofluid can be significantly decreased. To reinforce this hypothesis, we estimated the thermal conductivity (diffusivity) of InP nanocrystals using a theory with a phenomenological basis [34]. This theory incorporates the intrinsic size effect on phonon velocity and mean free path, as well as surface scattering of phonons. According to this theory, the thermal conductivity of a nanostructure is given by:

$$\frac{k_L}{k_b} = p\exp\left(-\frac{l_0}{L}\right)\left[\exp\left(\frac{1-a}{L/L_0-1}\right)\right]^{3/2} \quad (6)$$

where k_L is the thermal conductivity of the nanostructure, k_b is the thermal conductivity of the bulk material, L is the characteristic size of the nanostructure, L_0 [=2(3−f)σ] is the critical size when almost all atoms of the crystal are located on its surface, l_0 is the phonon mean path at room temperature, σ is the molecular/atomic diameter and $f = 0$ for nanoparticles. Parameter $a = 1 + \frac{2}{3} S_v R^{-1}$ where S_v is the vibrational entropy of melting and R (=8.31441 J mol^{-1} K^{-1}) is the universal gas constant. Parameter p is related to the surface roughness η via the relation $p = 1$–$10\,\frac{\eta}{L}$ so that $p = 1$ corresponds to a smooth surface and $p = 0$ to a very rough surface. The veracity of Eq. (6) has been demonstrated in previous work for ultrathin films, nanowires and semiconductor nanoparticles [23, 34].

Table 2 Calculated values of the thermal conductivity (using Eq. 6) and diffusivity (using $D_L = k_L/pC_p$) of InP nanoparticles with different sizes

L/nm	$k_L/10^{-4}$ J s^{-1} cm^{-1} K^{-1}	$D_L/10^{-4}$ cm^2 s^{-1}
Bulk	6,800	4,300.00
3.0	0.02	0.12
4.0	3.69	2.34
4.6	*8.86*	*4.96*
5.0	13.54	8.57
6.0	28.55	18.00

The related parameters used in Eq. (6) to estimate the k_L of InP nanocrystals are as follows: for InP, $k_b = 0.68$ - J s^{-1} cm^{-1} K^{-1} [35], $p = 0.07$ optimized value, $L =$ 4.6 nm experimental value, $l_o = 4.52$ nm [36], $S_v =$ 50.30079 [37] and $\sigma = 0.2542$ nm [38]. With the results of thermal conductivity k_L, it is possible to obtain the thermal diffusivity of InP nanoparticles trough $D_L = k_L/pC_p$, where p is the density and C_p the specific heat capacity of bulk InP. The results of thermal conductivities and diffusivity obtained of InP with different nanometric sizes are summarized in Table 2. The results show effectively that the D_L is smaller than the corresponding bulk value and than that of the toluene. D_L also decreases with decreasing of size particle. This would result in negative enhancements in the effective thermal diffusivity of nanofluids containing very small InP particles. Recent experimental results from the decrease in the thermal diffusivity of InP with size reduction [39] validate our calculus.

The size-dependent transport thermal from Eq. (6) was incorporate into the geometric mean of the thermal conductivity of the mixture of solid nanoparticles in a liquid [40] to estimate the thermal conductivity (diffusivity) of the semiconductor nanofluids in function on the content of particles:

$$\frac{k_N}{k_l} = \left(\frac{k_L}{k_l}\right)^{\phi} \tag{7}$$

where k_N is the thermal conductivity of the nanofluid, k_l is the is the thermal conductivity of the base fluid (toluene), k_L is the thermal conductivity of the nanoparticle and ϕ is the volume fraction (mass percentage). With the results of k_N, it is possible to obtain the thermal diffusivity of semiconductor nanofluids trough $D_N = k_N/pC_p$. In Fig. 6 are annexed the results obtained using Eq. (7) of the thermal diffusivity of semiconductor nanofluids with different percentage mass. The figure shows that the data are reasonably well predicted and that the thermal diffusivity (calculated and experimental) of 4.6 nm InP nanofluids is lower than the base fluid in all concentrations, so that the thermal diffusivity enhancement in InP nanofluids is negative. We attribute this decrease to the thermal diffusivity of nanoparticles being smaller than the thermal diffusivity of the toluene, thus validating our hypothesis. The calculated values give a nearly linear relationship between the thermal diffusivity and the percentage mass of InP nanoparticles. For greater percentages, higher decrease in thermal diffusivity is observed. It is noteworthy that the calculated values are more negative than the corresponding experimental data, especially when the concentration of nanoparticles is greater, suggesting that Eq. (7) underestimated the thermal diffusivity of the nanofluids. From these results and the analysis of the TEM image, we ascribe this anomalous variation mainly to the observed clustering of InP nanoparticles in the nanofluids.

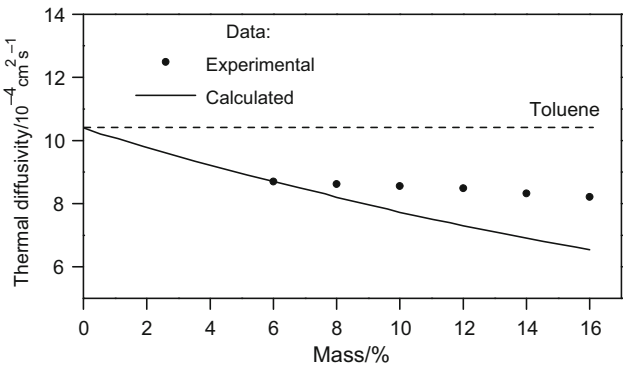

Fig. 6 Thermal diffusivity of nanofluids consisting of 4.6 nm InP nanoparticles in toluene. The points represent experimental data of this work. The *solid curve* represents the predictions using Eq. (4), and the dashed curve represents the thermal diffusivity of toluene for comparison

The contribution of the clustering of semiconductor nanoparticles in the thermal diffusivity of the nanofluids is not clear at the moment. However, the formation of clustering can create particle-liquid-particle pathways with lower thermal resistances and thereby have a positive effect on the thermal diffusivity of the nanofluid. This is because in the clustering the nanoparticles are separated by very small distances ~1–2 nm (Fig. 2); necessary and sufficient condition to ensure that the phonons (heat) initiated in one nanoparticle can persist in the liquid, and it get transmitted efficiently to another nanoparticle helping to enhanced the thermal diffusivity of the nanofluid [41]. Then, it would be predicted expected that well-dispersed InP nanoparticles in toluene would result in semiconductor nanofluids with a diffusivity more negative compared to nanofluids containing clustering of InP nanoparticles, as shown by the results calculated of Fig. 6. For example, it may be noted that the decrease calculated of the thermal diffusivity of the nanofluid with percentage mass 16 % with well-dispersed nanoparticles is ~37 %, while for the same percentage mass of InP clustering, we have an experimental decrease in only ~21 %. With the degree of clustering, minor decrease in the thermal diffusivity in the nanofluids semiconductors is expected.

Thus, while metallic and nonmetallic nanoparticles play an important role in positive increment of thermal diffusivity for base fluids, the InP semiconductor nanoparticles confined at nanometric scale should contribute to decrease the thermal diffusivity. Certainly, it demonstrates the effect of the presence of semiconductor nanoparticles and the concentration on the reduction in diffusivity in the semiconductor nanofluid. Besides nanoparticle type (metallic, nonmetallic or semiconductor) and size, the concentration of semiconductor nanoparticles can play an important role on liquid's thermal properties.

Conclusions

We have measured the thermal diffusivity of semiconductor nanofluids containing InP nanocrystals with different concentrations (6.0–16.0 mass/%). Nanocrystals were obtained by using chemical procedure. Formation of semiconductor crystals with average 4.6 nm was verified through optical absorption spectra, TEM and HRTEM analysis. Our results indicate that the thermal diffusivity of toluene remarkably decreases due to the presence of InP nanocrystals. Smaller thermal diffusivities were obtained for nanofluids containing higher concentrations of nanocrystals. The decrease in thermal diffusivity of nanofluids is consequence of decrease in the thermal diffusivity of the InP nanocrystals themselves. The measured thermal diffusivity of the semiconductor nanofluids is less

negative than those predicted with existing model. This variation of thermal diffusivity was mainly due to the presence of nanoparticles clustering in nanofluids.

Acknowledgements The authors are thankful to the Mexican Agencies, ICyTDF, CONACYT, COFAA-IPN, SIP-IPN for financial supports.

References

1. Choi SUS. Enhancing thermal conductivity of fluids with nanoparticles. In: Singer DA, Wang HP, editors. Developments and applications of non-newtonian flows. New York: American Society of Mechanical Engineers; 1995. p. 99–105.
2. Dan L, Wenjun F, Huiqin W, Chao G, Renyi Z, Keke C. Gold/oil nanofluids stabilized by a gemini surfactant and their catalytic property. Ind Eng Chem Res. 2013;52:8109–13.
3. Wong KV, De Leon O. Application of nanofluids: current and future. Adv Mech Eng. 2010; 2010: Article ID 519659: 1–11.
4. Taylor R, Coulombe S, Otanicar T, Phelan P, Gunawan A, Lv W, Rosengarten G, Prasher R, Tyagi H. Small particles, big impacts; a review of the diverse applications of nanofluids. J Appl Phys. 2013;113:011301.
5. Wang X-Q, Mujumdar AS. A review on nanofluids-part II: experimental and applications. Braz J Chem Eng. 2008;25:631–48.
6. Kakaç S, Pramuanjaroenkij A. Review of convective heat transfer enhancement with nanofluids. Int J Heat Mass Tran. 2009;52:3187–96.
7. Wang X-Q, Mujumdar AS. A review on nanofluids-part I: theoretical and numerical investigations. Braz J Chem Eng. 2008;25:613–30.
8. Barbés B, Páramo R, Blanco E, Casanova C. Thermal conductivity and specific heat capacity measurements of CuO nanofluids. J Therm Anal Calorim. 2014;115:1883–91.
9. Wang X-Q, Mujumdar AS. Heat transfer characteristics of nanofluids: a review. Int J Therm Sci. 2007;46:1–19.
10. Kwek D, Crivoi A, Duan F. Effects of temperature and particle size on the thermal property measurements of Al_2O_3-water nanofluids. J Chem Eng Data. 2010;55:5690–5.
11. Shima PD, Philip J, Raj B. Synthesis of aqueous and nonaqueous iron oxide nanofluids and study of temperature dependence on thermal conductivity and viscosity. J Phys Chem C. 2010;114:18825–33.
12. Xie H, Chen L. Review on the preparation and thermal performances of carbon nanotube containing nanofluids. J Chem Eng Data. 2011;56:1030–41.
13. Baby TT, Sundara R. Synthesis and transport properties of metal oxide decorated grapheme dispersed nanofluids. J Phys Chem C. 2011;115:8527–33.
14. Amiri A, Shanbedi M, Eshghi H, Heris SZ, Baniadam M. Highly dispersed multiwalled carbon nanotubes decorated with Ag nanoparticles in water and experimental investigation of the thermophysical properties. J Phys Chem C. 2012;116: 3369–75.
15. Paul G, Chopkar M, Manna I, Das PK. Techniques for measuring the thermal conductivity of nanofluids: a review. Renew Sust Energ Rev. 2010;14:1913–24.
16. Jiménez-Pérez JL, Sánchez-Ramírez JF, Cruz-Orea A, Gutiérrez Fuentes R, Cornejo Monroy D, López-Muñoz GA. Heat transfer enhanced in water containing TiO2 nanospheres. J Nano Res. 2010;9:55–60.
17. Jiménez-Pérez JL, Cruz-Orea A, Sánchez-Sinencio JF, Sánchez-Sinencio F, Martínez-Pérez I, López Muñoz GA. Thermal characterization of nanofluids with different solvents. Int J Thermophys. 2009;30:1227–33.
18. Gutiérrez Fuentes R, Pescador Rojas JA, Jiménez-Pérez JL, Sánchez Ramírez JF, Cruz-Orea A, Mendoza-Álvarez JG. Study of thermal diffusivity of nanofluids with bimetallic nanoparticles with Au(core)/Ag(shell) structure. Appl Surf Sci. 2008;255:781–3.
19. Gutiérrez Fuentes R, Sánchez-Ramírez JF, Jiménez Pérez JL, Pescador Rojas JA, Ramón-Gallegos E, Cruz-Orea A. Thermal diffusivity determination of protoporphyrin IX solution mixed with gold metallic nanoparticles. Int J Thermophys. 2007;28:1048–55.
20. Cahill DG, Ford WK, Goodson KE, Mahan GD, Majumdar A, Maris HJ, Merlin R, Phillpot SR. Nanoscale thermal transport. J Appl Phys. 2003;93:793–818.
21. Liu W, Asheghi M. Phonon-boundary scattering in ultrathin single-crystal silicon layers. Appl Phys Lett. 2004;84:3819–21.
22. Li D, Wu Y, Kim P, Shi L, Yang P, Majumdar A. Thermal conductivity of individual silicon nanowires. Appl Phys Lett. 2003;83:2934–6.
23. Teja AS, Beck MP, Yuan Y, Warrier P. The limiting behavior of the thermal conductivity of nanoparticles and nanofluids. J Appl Phys. 2010;107:114319.
24. Michalet X, Pinaud F F, Bentolila LA, Tsay JM, Doose S, Li JJ, Sundaresan G, Wu AM, Gambhir SS, Weiss S. Quantum dots for live cell, in vivo imaging, and diagnostic. Science. 2005; 307: 438–44.
25. Kairdolf BA, Smith AM, Stokes TH, Wang MD, Young AN, Nie S. Semiconductor quantum dots for bioimaging and biodiagnostic applications. Ann Rev Anal Chem. 2013;6:143–62.
26. Bindhu CV, Harilal SS, Nampoori VPN, Villabhan CPG. Thermal diffusivity measurements in organic liquids using transient thermal lens calorimetry. Opt Eng. 1998;37:2791–4.
27. Moreira LM, Carvalho EA, Bell MJV, Anjos V, Sant'Ana AC, Alves APP, Fragneaud B, Sena LA, Archanjo BS, Achete CA. Thermo-optical properties of silver and gold nanofluids. J Therm Anal Calorim. 2013;114:557–64.
28. Li L, Reiss P. One-pot synthesis of highly luminescent InP/ZnS nanocrystals without precursor injection. J Am Chem Soc. 2008;130:11588–9.
29. Shen J, Lowe RD, Snook RD. A model for cw laser induced mode-mismatched dual-beam thermal lens spectrometry. Chem Phys. 1992;165:385–96.
30. Mićić OI, Cheong HM, Fu H, Zunger A, Sprague JR, Mascarenhas A, Nozik AJ. Size dependent spectroscopy of InP quantum dots. J Phys Chem. 1997;101:4904–12.
31. Byun HJ, Lee JC, Yang H. Solvothermal synthesis of InP quantum dots and their enhanced luminescent efficiency by post-synthetic treatments. J Colloid Interface Sci. 2011;355:35–41.
32. Ponomareva I, Srivastava D, Menon M. Thermal conductivity in thin silicon nanowires: phonon confinement effect. Nano Lett. 2007;7:1155–9.
33. George SD, Radhakrishnan P, Nampoori VPN, Vallabhan CPG. Thermal characterization of intrinsic and extrinsic InP using photoacoustic technique. J Phys D Appl Phys. 2003;36:990–3.
34. Liang LH, Li B. Size-dependent thermal conductivity of nanoscale semiconducting system. Phys Rev B. 2006;73:153303–4.
35. http://www.ioffe.ru/SVA/NSM/Semicond/InP/thermal.html.
36. Kang S, Myles CW. Effect of deep level impact ionization on avalanche breakdown in semiconductor p–n junctions. Phys Stat Sol A. 2000;181:219–29.
37. Zhang Z, Zhao M, Jiang Q. Melting temperatures of semiconductor nanocrystals in the mesoscopic size range. Semicond Sci Technol. 2001;16:L33–5.

38. Liang LH, Shen CM, Chen XP, Liu WM, Gao HJ. The size-dependent phonon frequency of semiconductor nanocrystals. J Phys Condens Matter. 2004;16:267–72.
39. Srinivasan R, Ramachandran K. Thermal diffusion in nanostructured porous InP. Bull Mater Sci. 2008;31:863–8.
40. Turian RM, Sung DJ, Hsu FL. Thermal conductivity of granular coals, coal-water mixtures and multi-solid/liquid suspensions. Fuel. 1991;70:1157–72.
41. Eapen J, Li J, Yip S. Probing transport mechanisms in nanofluids by molecular dynamics simulations. 18th National and 7th ISHMT–ASME Heat and Mass Transfer Conference, IIT Guwahati, India, 2006. Paper No. HMT-2006-C339.